# 常時地震活動・余震・誘発地震の予測能力と評価

尾形良彦
統計数理研究所, 地震研究所

$$P(M \mid A,B,C,\cdots,S) = \frac{1}{1+\left(\frac{1}{P_A}-1\right)\left(\frac{1}{P_B}-1\right)\left(\frac{1}{P_C}-1\right)\cdots\left(\frac{1}{P_S}-1\right)\Big/\left(\frac{1}{P_0}-1\right)^{N-1}} \approx P_0 \cdot \frac{P_A}{P_0}\frac{P_B}{P_0}\frac{P_C}{P_0}\cdots\frac{P_S}{P_0}$$

$$確率利得 = \frac{異常現象が大地震の前兆である確率}{大地震の基礎確率}$$

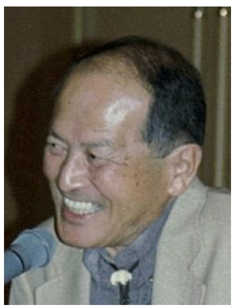

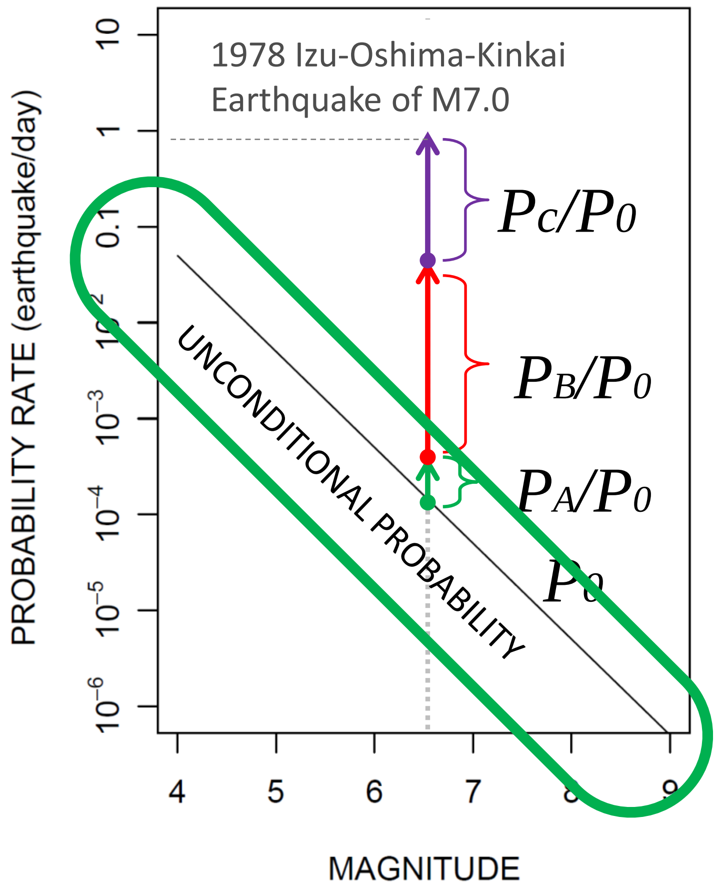


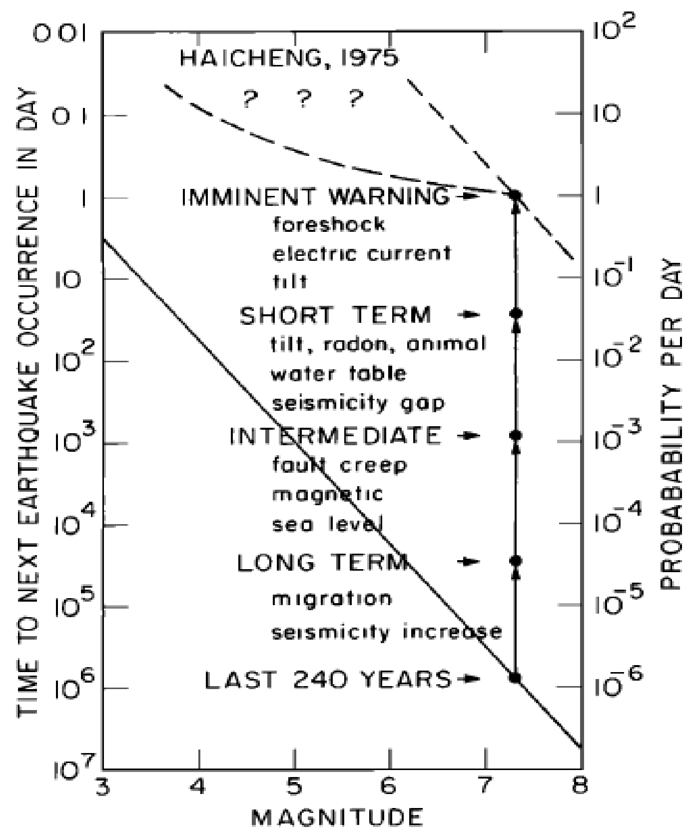

# Official **Annual** earthquake predictions made by China Earthquake Administration

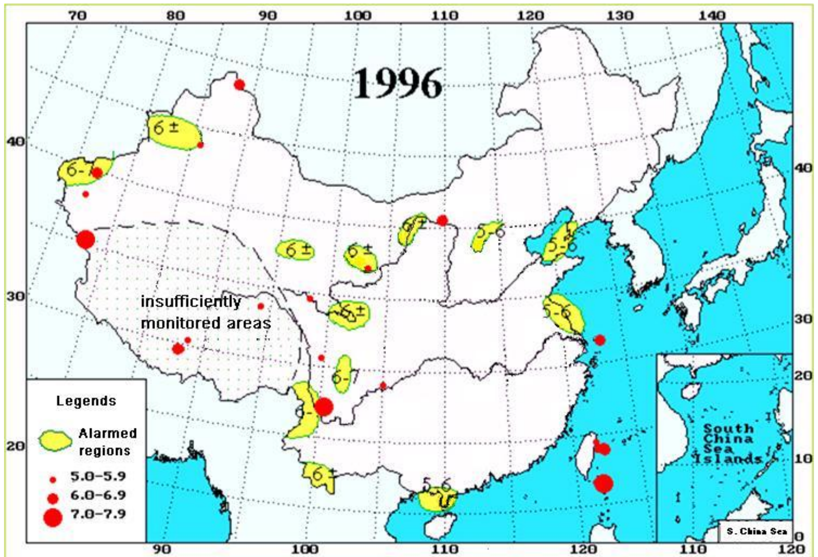


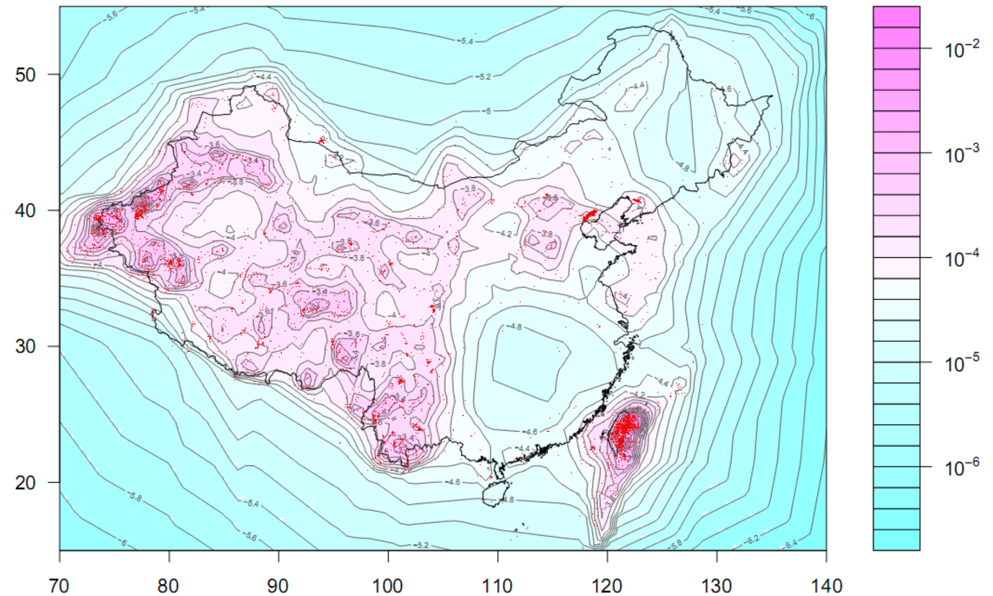

Chinese annual earthquake predictions in 1996.
The alarmed regions are marked in yellow and the earthquakes with M5 and above are represented by red dots. The numbers on the alarmed regions are the magnitude ranges of the expected future earthquakes.

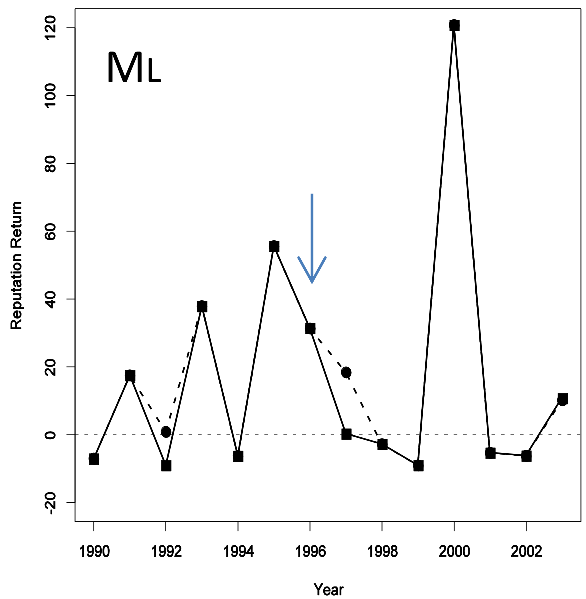


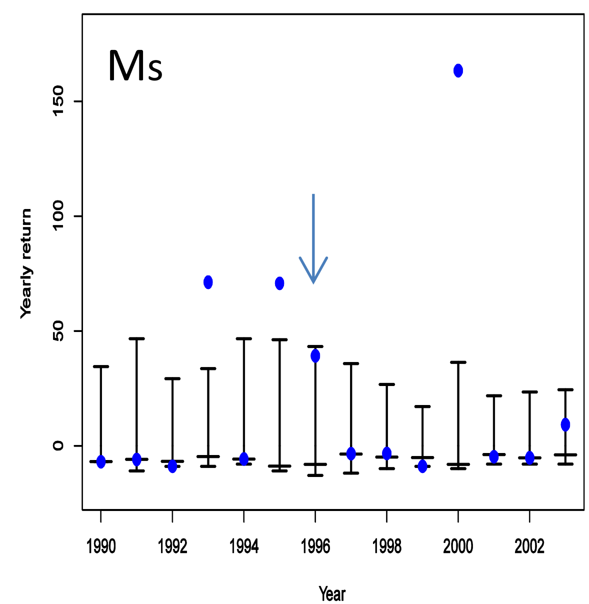


**Gambling Scores analysed by Zhuang and Jiang (2012, Tectonophysics)**

3ヵ月予測第5ラウンド lov.1.2010 – Jan.31.2011

日本列島

M ≥ 5.0／3ヵ月

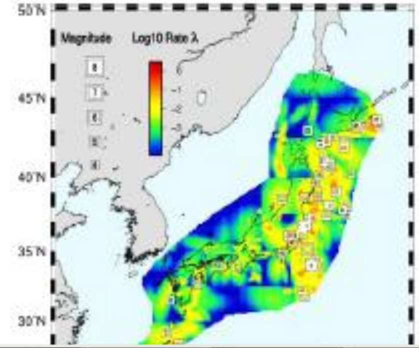

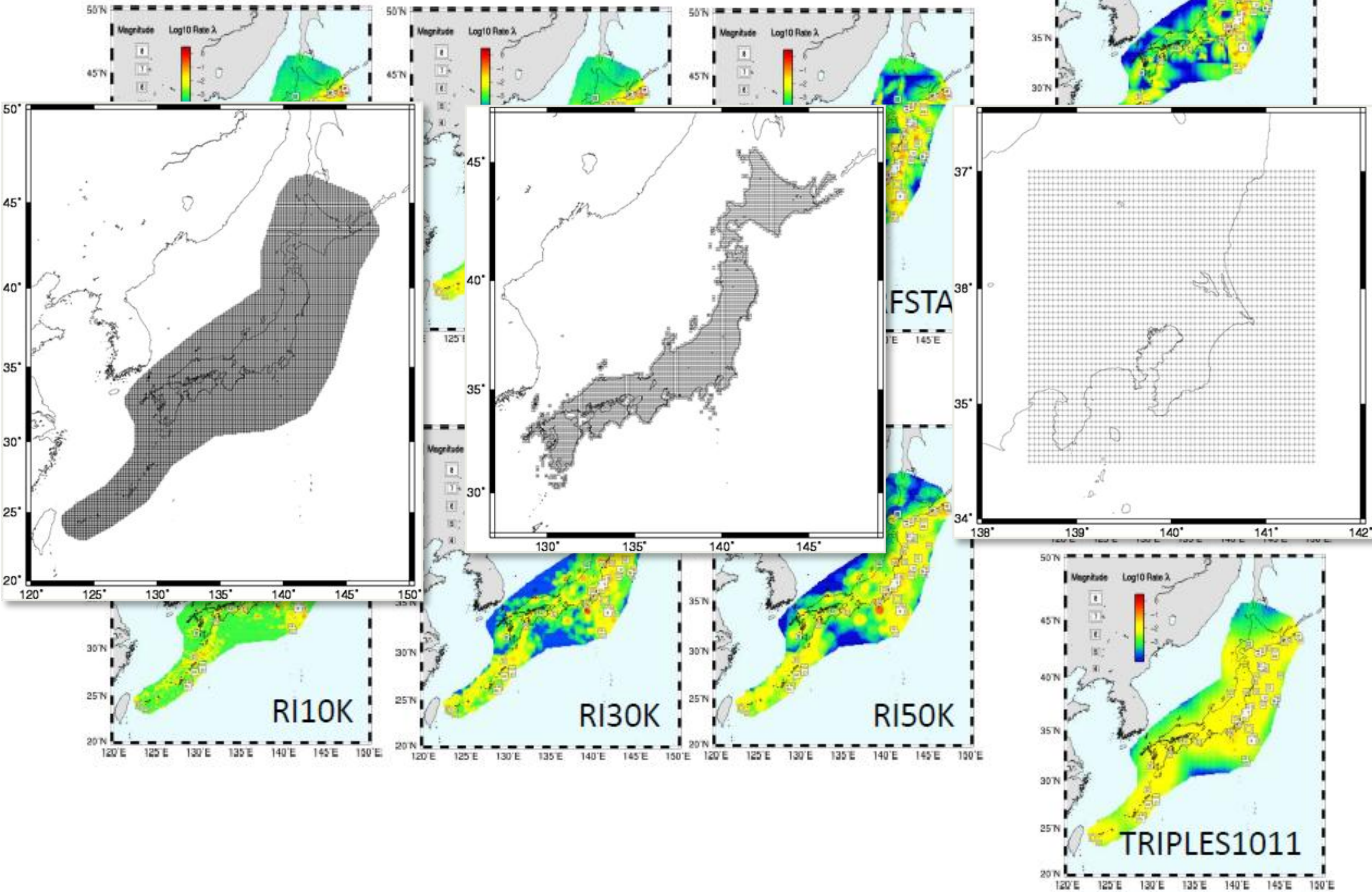

# 時間･空間･マグニチュード →4D bins

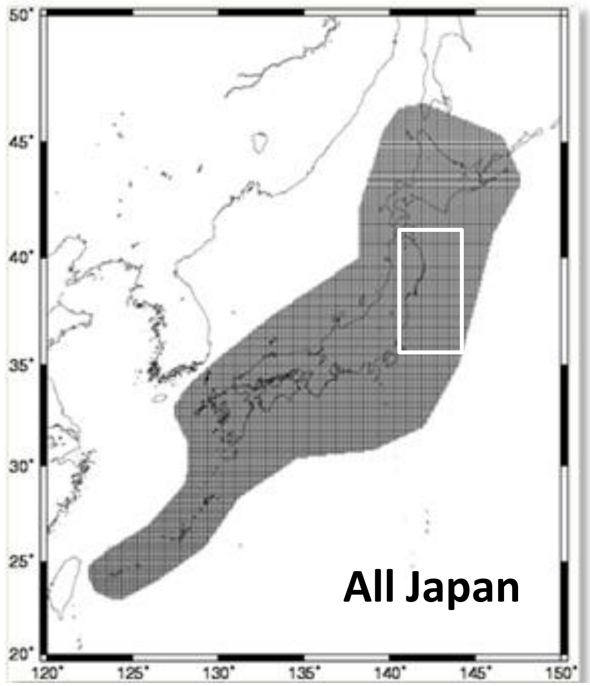


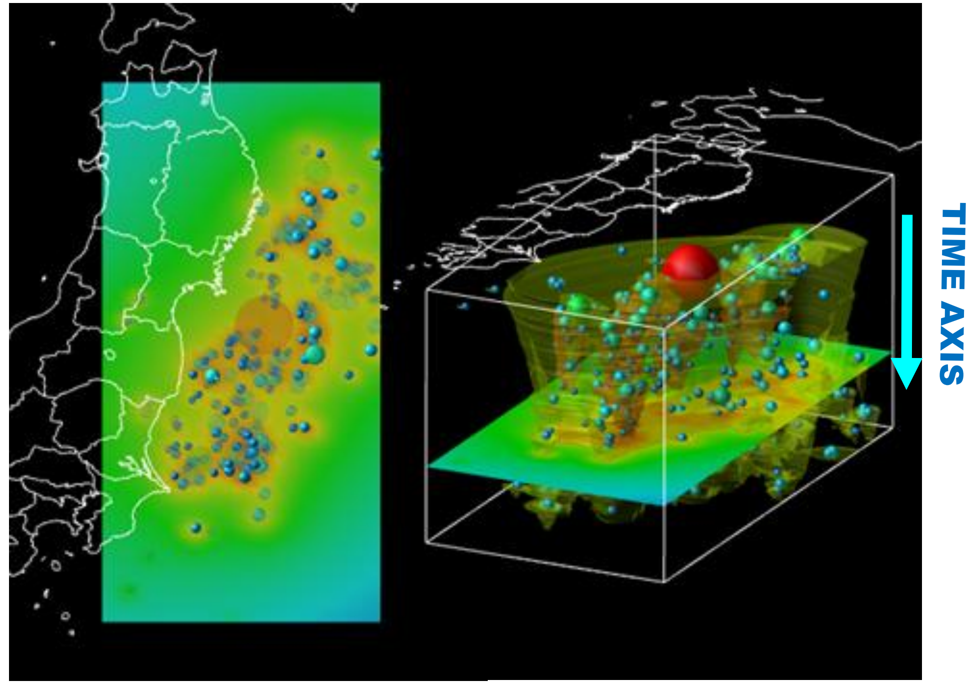


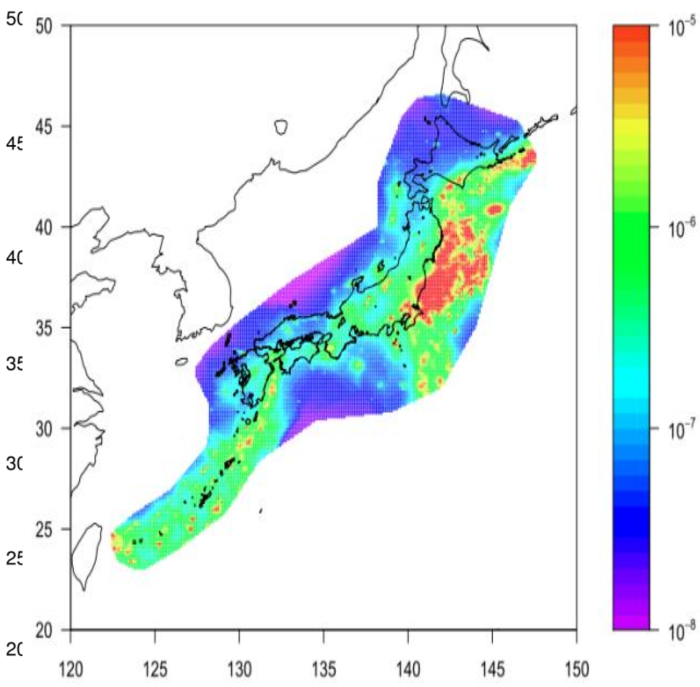

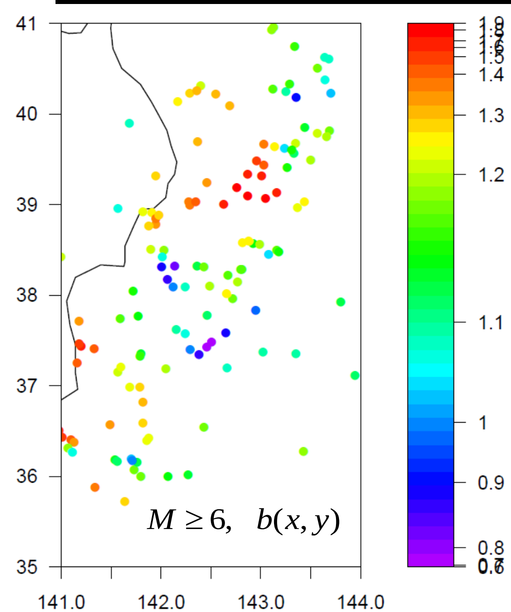


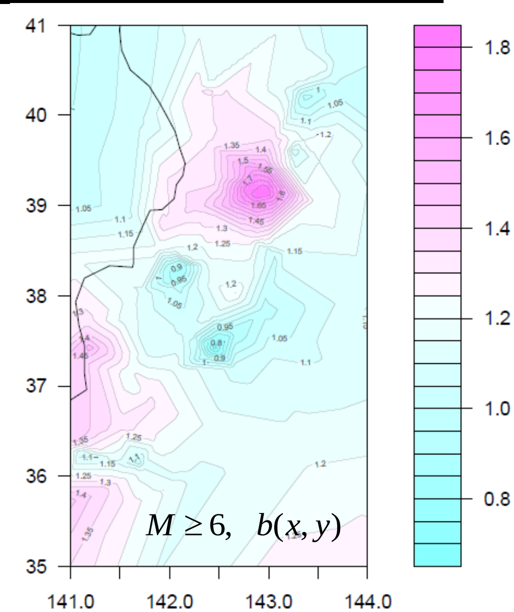

# 統計モデルと予測

Bin ← (time)x(space)x(magnitude)

| bins | 1 | 2 | 3 | ・・・ | n | sums |
|---|---|---|---|---|---|---|
| forecasts | $p_1$ | $p_2$ | $p_3$ | ・・・ | $p_n$ | $\Sigma\ p_i=1,\quad p_i>0$ |
| #quakes | $m_1$ | $m_2$ | $m_3$ | ・・・ | $m_n$ | $\Sigma\ m_i=N,\quad m_i \geqq 0$ |
| relative frequency | $\nu_1$ | $\nu_2$ | $\nu_3$ | ・・・ | $\nu_n$ | $\Sigma\ \nu_i=1,\ \nu_i=m_i/N$ |

$\approx f(x_1,x_2,\cdots x_n)dx_1dx_2\cdots dx_n$

$\approx g(x_1,x_2,\cdots x_n)dx_1dx_2\cdots dx_n$

- Probability that the model $\mathbf{p}=(p_1,p_2,\cdots,p_n)$ realizes the frequency $\mathbf{v}=(\nu_1,\nu_2,\cdots,\nu_n)$

$$W = Probability = \frac{n!}{m_1!m_2!\cdots m_n!}p_1^{m_1}p_2^{m_2}\cdots p_n^{m_n}$$

確率予測 pで実現頻度ν が
得られる確率W
＝予測の評価

$$\approx e^{N\sum_i \nu_i \ln \frac{p_i}{\nu_i}} = e^{N\sum_i \nu_i \ln p_i - N\sum_i \nu_i \ln \nu_i}$$

**Relative entropy** **log-likelihood**

$$\propto \exp\left[\int_{V^n} g(x_1,x_2,\cdots,x_n)\ln\left\{\frac{f(x_1,x_2,\cdots,x_n)}{g(x_1,x_2,\cdots,x_n)}\right\}dx_1dx_2\cdots dx_n\right] = C\cdot\exp\left[E_g\{\ln f(X_1,X_2,\cdots,X_n)\}\right]$$

| | 対数尤度 | 尤度 | 相対尤度 | 正規化尤度 |
|---|---|---|---|---|
| **Models** | **Δ ln L** | **Likelihood** | **Likelihood0** | **density** |
| 1 | **325.82** | **3.1756E+141** | **1** | **0.521558** |
| 2 | 325.39 | 2.0658E+141 | 0.6505091 | 0.339278 |
| 3 | 324.29 | 6.8763E+140 | 0.2165357 | 0.112936 |
| 4 | 322.83 | 1.5969E+140 | 0.0502874 | 0.026228 |
| 5 | 282.07 | 3.1728E+122 | 9.991E-20 | 5.21E-20 |
| 6 | 268.16 | 2.8867E+116 | 9.09E-26 | 4.74E-26 |
| 7 | 247.61 | 3.4329E+107 | 1.081E-34 | 5.64E-35 |
| 8 | 252.67 | 5.4099E+109 | 1.704E-32 | 8.89E-33 |
| 9 | 229.10 | 3.1395E+99 | 9.886E-43 | 5.16E-43 |
| 10 | **0.00** | **1** | 1.85E-110 | 9.6E-111 |
| **sum** | | 6.0887E+141 | 1.9173322 | 1 |

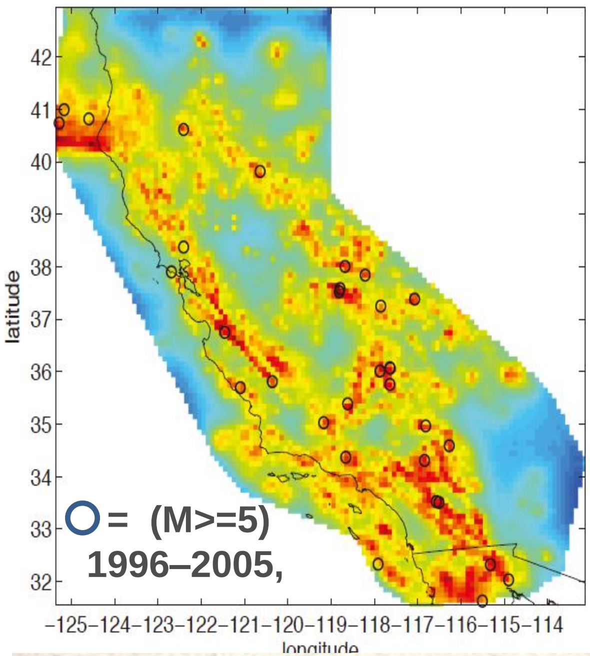


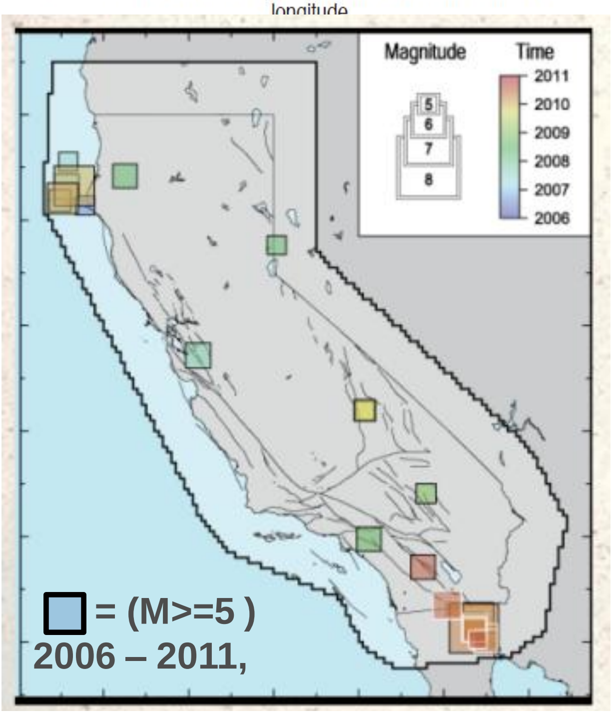


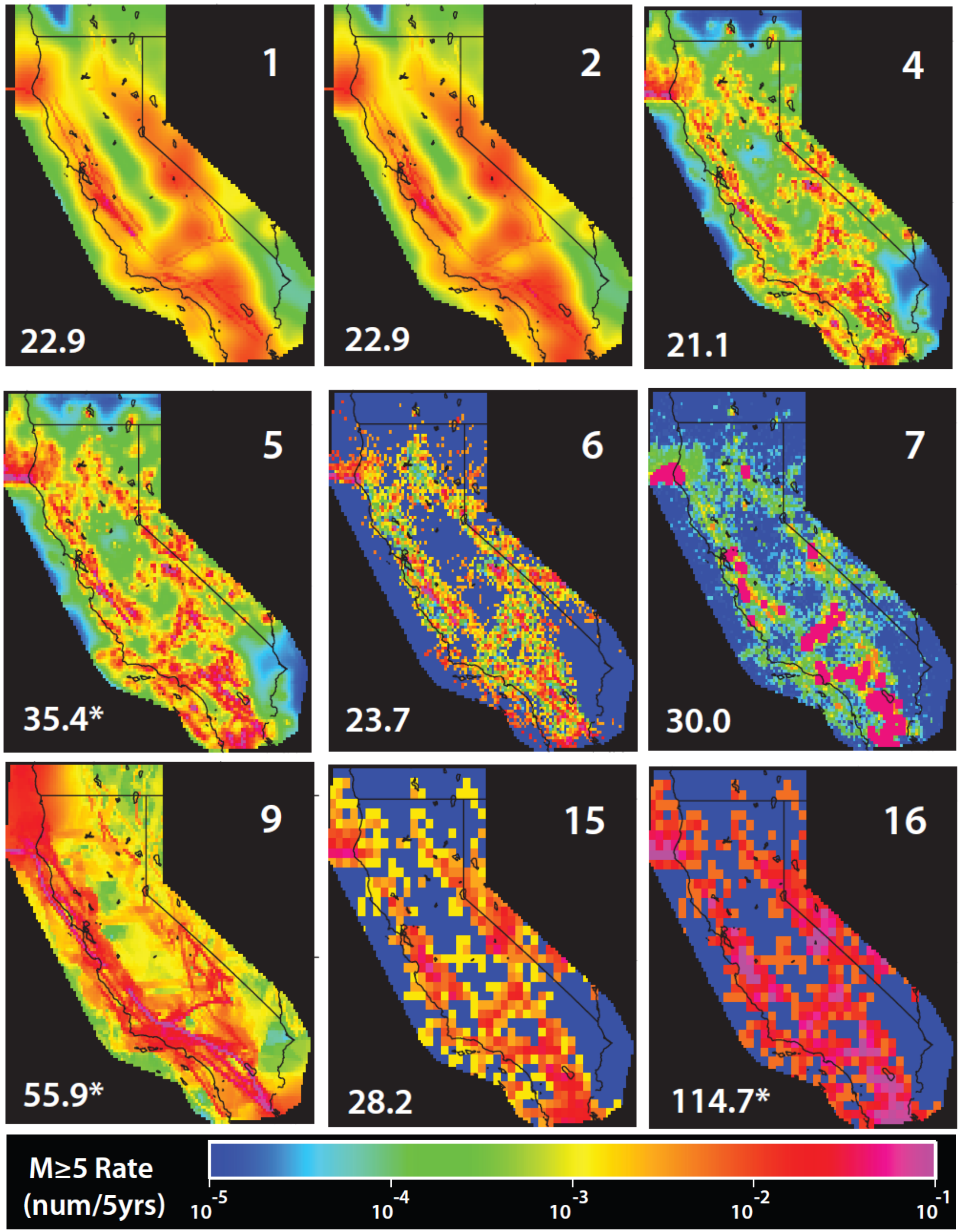


31 earthquakes, 20 main shocks

# Gutenberg-Richter model × Background rate of HIST-ETAS model

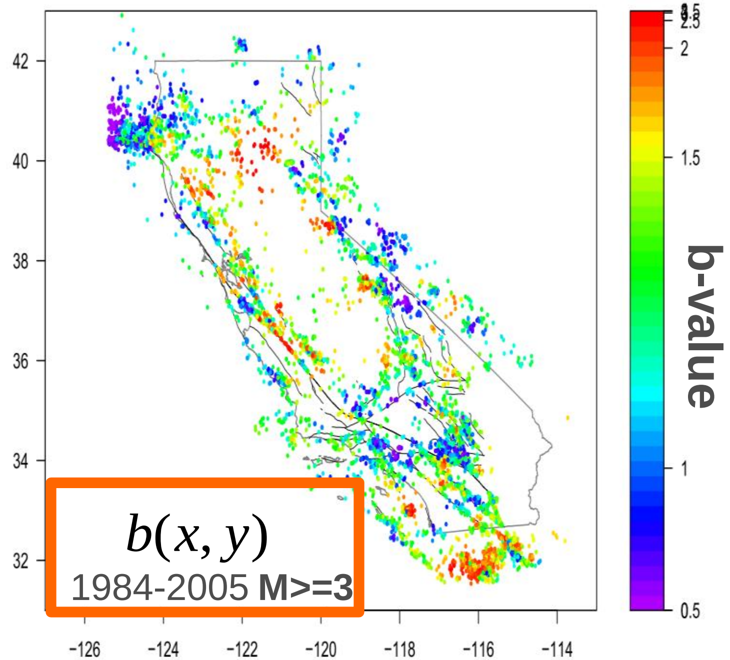


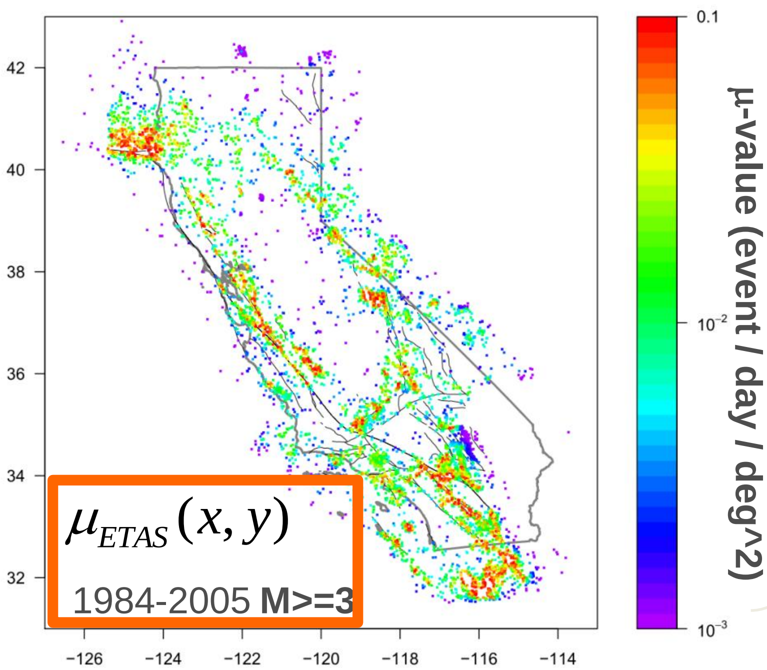


$$\lambda(t, x, y) = \mu(x, y) + \sum_{\{j;\, t_j < t\}} \frac{K(x, y)}{(t - t_j + c)^{p(x,y)}} \times \left[ \frac{(x - x_j, y - y_j)\, S_j\, (x - x_j, y - y_j)^t}{e^{\alpha(x,y)(M_j - M_c)}} + d \right]^{-q(x,y)}$$

$$\int_{5.0}^{\infty} dM \int_{2006}^{2011} dt \iint_{PIXEL} dxdy\; 10^{-b(x,y)M}\; \mu_{ETAS}(x, y)$$

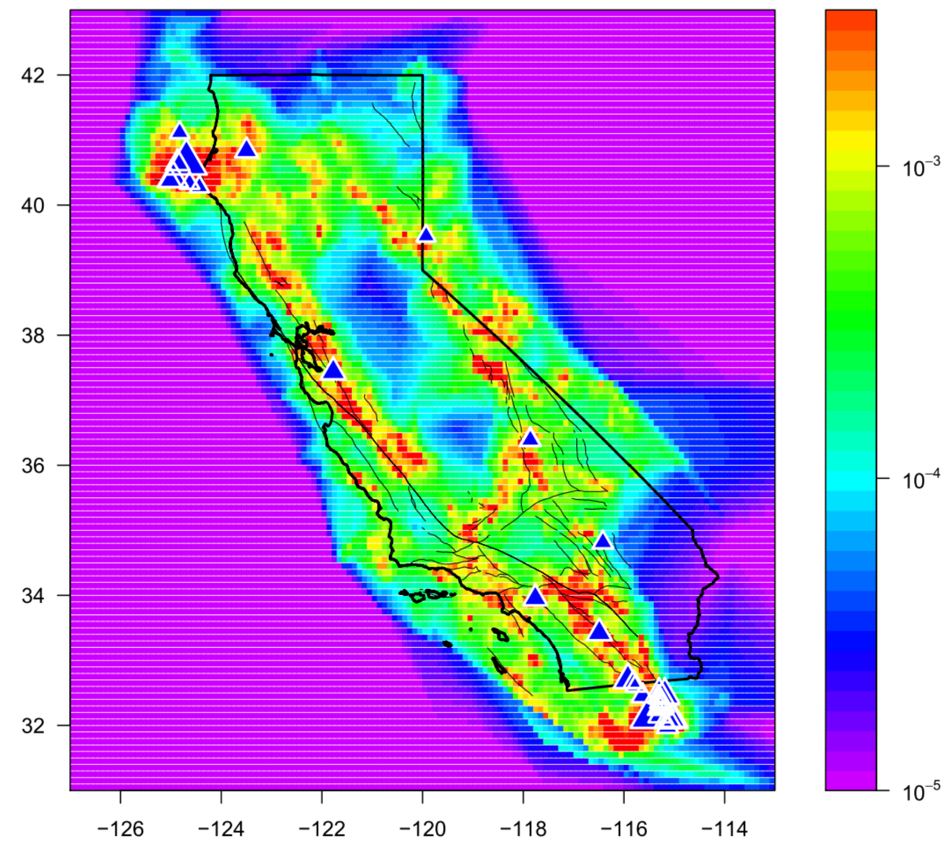

**1926-1995 の期間の M>=5.0 の地震データから推定**

☆ = **1996 – 2009**の期間で起きた **M>= 6.7** の大地震

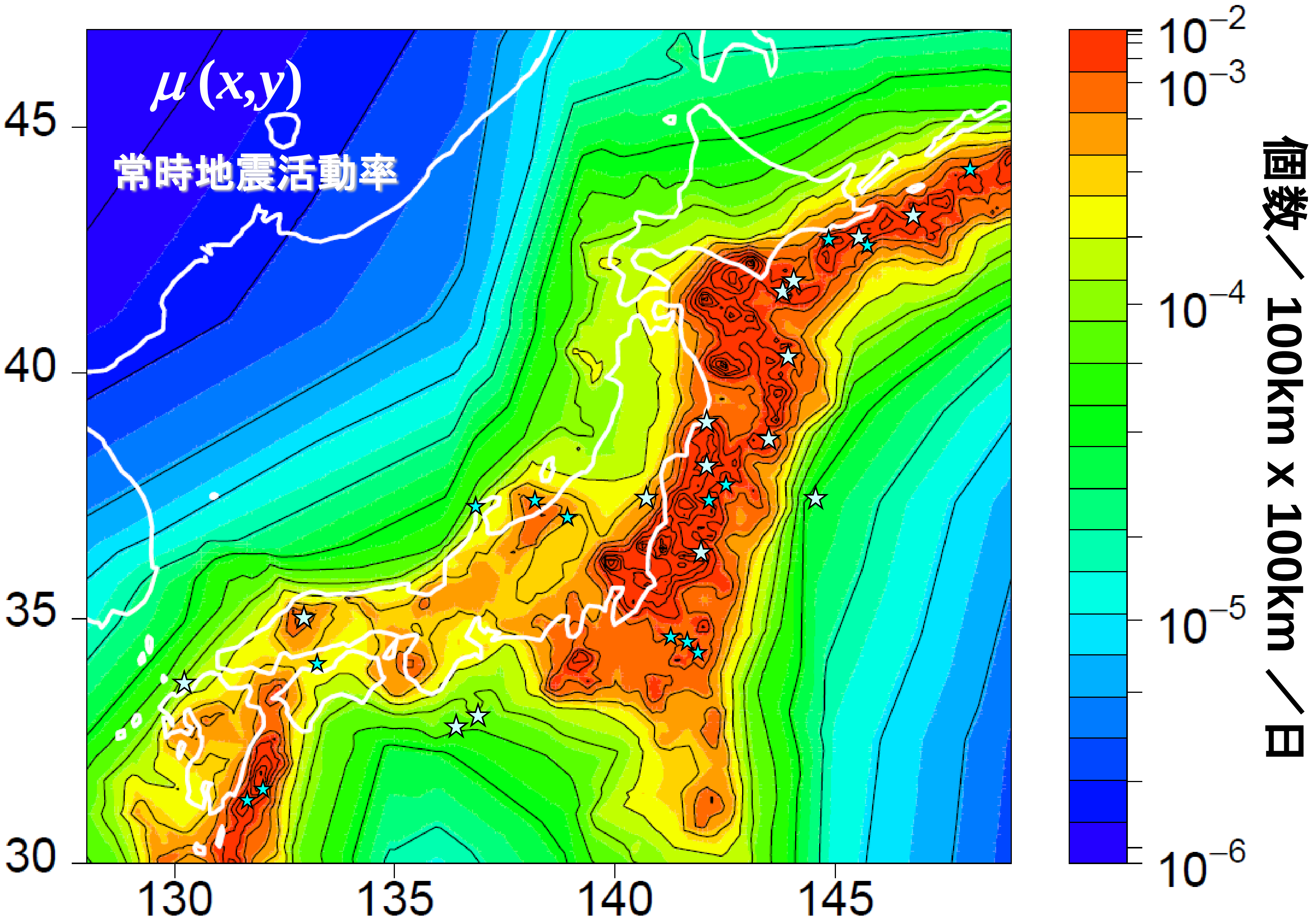

# How is the AIC derived?

Assume that the Present Data $\mathbf{x} = (x_1, x_2, \ldots, x_n)$ and Future Data $\mathbf{y} = (y_1, y_2, \ldots, y_n)$ are from the same probability law. Consider a set of parametric model $\{f(\mathbf{y} \mid \theta); \theta \in \Theta\}$

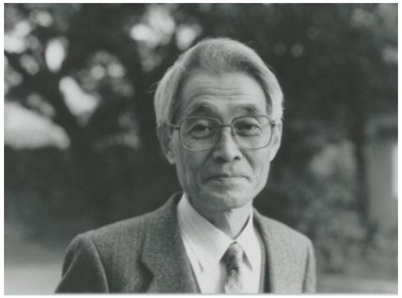

**A. Plug-in Type Predictor:** $f(\mathbf{y} \mid {}_p\hat{\theta}(\mathbf{x}))$

**Expected Negentropy of the predictor**

$$E_{\mathbf{x}}\left[E_{\mathbf{y}}\left\{\ln \frac{g(\mathbf{Y})}{f(\mathbf{Y} \mid {}_p\hat{\theta}(\mathbf{X}))}\right\}\right] = E_{\mathbf{y}}[\ln g(\mathbf{Y})] - E_{\mathbf{x}}E_{\mathbf{y}}[\ln f(\mathbf{Y} \mid {}_p\hat{\theta}(\mathbf{X}))]$$

Future data **Y** available $\approx \quad const. - \ln f(\mathbf{Y} \mid \hat{\theta}(\mathbf{X}))$

Predictive log-likelihood of a model

Future data **Y** not available

$$\approx \quad const. - \ln f(\mathbf{X} \mid \hat{\theta}_p(\mathbf{X})) + p \quad \approx \frac{AIC}{2}$$

Predictive likelihood of a model $\propto \exp\left\{-\frac{AIC}{2}\right\}$

# 長期地震予測能力の評価 （野村,尾形, 2014, JpGU）

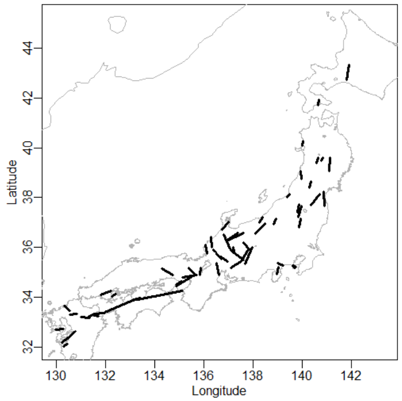


解析に用いた61活動区間の分布図

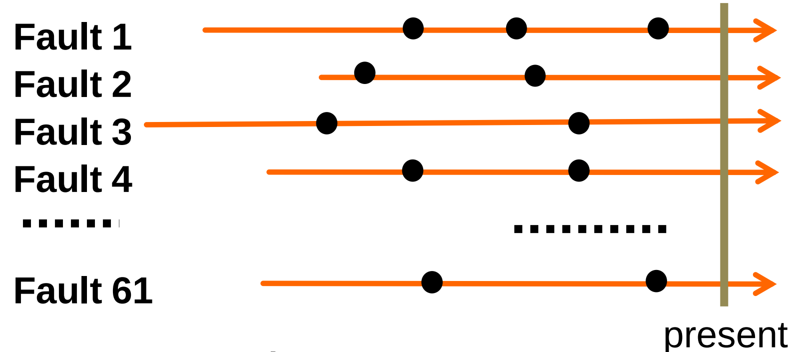


$$f(x;\mu,\alpha)=\sqrt{\frac{\mu}{2\pi\alpha^2x^3}}\exp\left\{-\frac{(x-\mu)^2}{2\mu\alpha^2x}\right\}$$

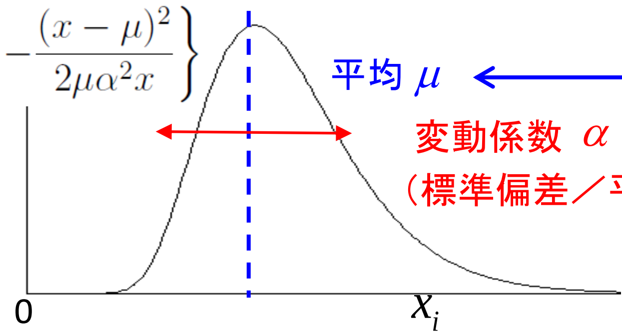


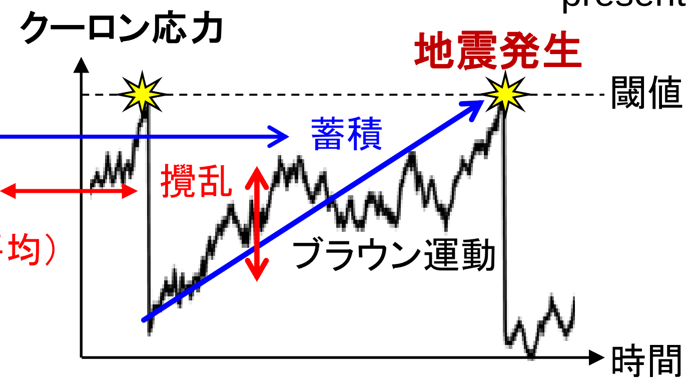


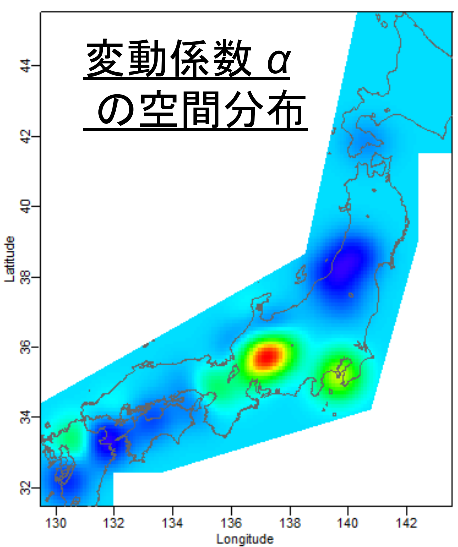


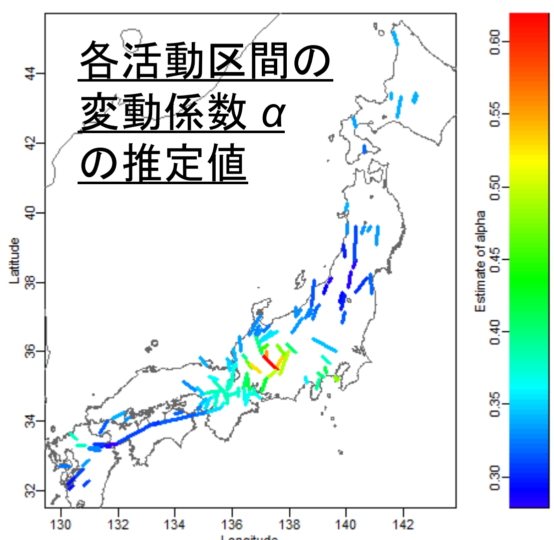


変動係数 **α**（範囲：**0.28〜0.62**、平均 **0.37**）の空間分布： **AIC = −26.6**

最尤推定量： **α ＝ 0.44** **AIC = −25.6**

地震調査委： **α ＝ 0.24** **AIC = 0.0**

J. Woessner, S. Hainzl, W. Marzocchi, M.J. Werner, A.M. Lombardi, F. Catalli, B. Enescu, M. Cocco, M.C. Gerstenberger, and S. Wiemer (2011, *JGR*)

A retrospective comparative forecast test on the 1992 Landers sequence.

**Table 2.** Number of Learning and Target Earthquakes and Focal Mechanisms Available in the Testing Region[a]

| Period | Relocated Events | | Events With Fault Plane Solution | |
|---|---|---|---|---|
| | $M_L \geq 0.1$ | $M_L \geq 3$ | $M_L \geq 0.1$ | $M_L \geq 4.5$ |
| $1984 < T_M$ | 38941 | 670 | 10102 | 15 |
| $T_M - T_M + 90d$ | 21647 | 1245 | 4354 | 31 |

[a] $T_M$ is the main shock time of the 1992 $M_L$ 7.3 Landers earthquake.

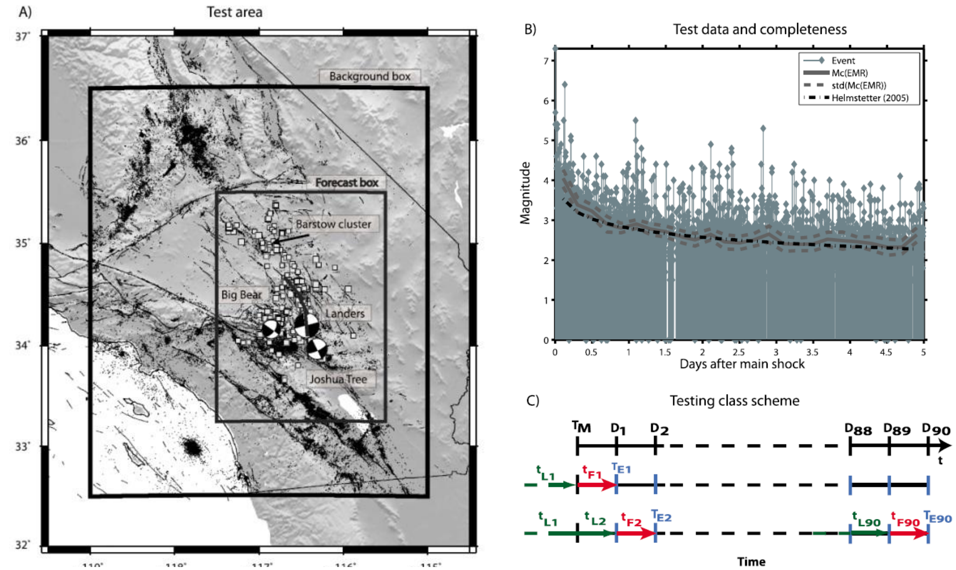


**Table 1.** Overview of the Forecast Models That Contributed Forecasts for the Retrospective Testing Experiment[a]

| | Model Type/ Model Name | Features | Total/Free Parameters | Modeler/Reference |
|---|---|---|---|---|
| 0 | STEP-0 generic STEP | $M_{th} = 6$ reference model | 6/0 | Woessner/*Gerstenberger et al.* [2005] |
| 1 | STEP-1 modified STEP | $M_{th} = 2.5$ | 6/6 | Woessner/*Gerstenberger et al.* [2005] |
| 2 | ETAS-1 | space-independent parameters stationary homogeneous bg. | 7/7 | Hainzl/*Hainzl et al.* [2008] |
| 3 | ETAS-2 | $K$ is space dependent stationary homogeneous bg. | 7/7 | Hainzl/*Hainzl et al.* [2008] |
| 4 | ETAS-3 | stationary heterogeneous bg. | 8/7 $q = 1.5$ | Lombardi/*Lombardi et al.* [2010] |
| 5 | ETAS-4 NETAS | nonstationary heterogeneous bg. | 9/8 $q = 1.5$ | Lombardi/*Lombardi et al.* [2006] |
| 6 | ETAS-5 | stationary heterogeneous bg. "effective parameters" | 6/0 | Werner/*Helmstetter et al.* [2006, 2007] |
| 7 | ETAS-6 | stationary heterogeneous bg. updating "effective parameters" | 6/5 | Werner/*Helmstetter et al.* [2006, 2007] |
| 8 | CRS-1 | space-dependent stressing rate nonuniform reference seismicity | 1/1 | Catalli/*Catalli et al.* [2008] |
| 9 | CRS-2 | stationary heterogeneous background | 4/1 $r$ not fix | Enescu/*Toda et al.* [1998] |
| 10 | CRS-3 | stress heterogeneity $CV$ stationary uniform bg. | 4/3 $t_a$ fix | Hainzl/*Hainzl et al.* [2009] |
| 11 | CRS-4 | stress heterogeneity $CV$ stationary uniform bg. poroelastic & coseismic | 4/3 $t_a$ fix | Hainzl/*Hainzl et al.* [2009] |

[a]The model number, the model class, first-order features, the number of total and free parameters, as well as the modeler and the reference(s) of the models are given. $M_{th}$ is a threshold magnitude that determines which earthquakes are used as triggering events in the STEP model.

**Table 6.** Joint Log Likelihood $LL_S$ and Probability Gain Per Earthquake Gain($S$) for All Models[a]

| Model | $LL_S$ | Gain($S$) | Rank |
|---|---|---|---|
| STEP-0 | −5187.40 | 1.00 | |
| STEP-1 | −4099.87 | 3.02 | 8 |
| ETAS-1 | −3160.40 | 7.86 | 4 |
| ETAS-2 | −3012.83 | 9.14 | 3 |
| ETAS-3 | −3708.66 | 4.50 | 6 |
| ETAS-4 | −3308.43 | 6.76 | 5 |
| ETAS-5 | −2905.26 | 10.19 | 1 |
| ETAS-6 | −2907.27 | 10.17 | 2 |
| CRS-1 | -inf | 0.00 | 11 |
| CRS-2 | −5351.49 | 0.85 | 10 |
| CRS-3 | −3932.49 | 3.58 | 7 |
| CRS-4 | −4298.86 | 2.47 | 9 |

[a]The probability gain is computed against the reference model STEP-0. The rank denotes the comparative ranking based on the spatial predictive power of the models.

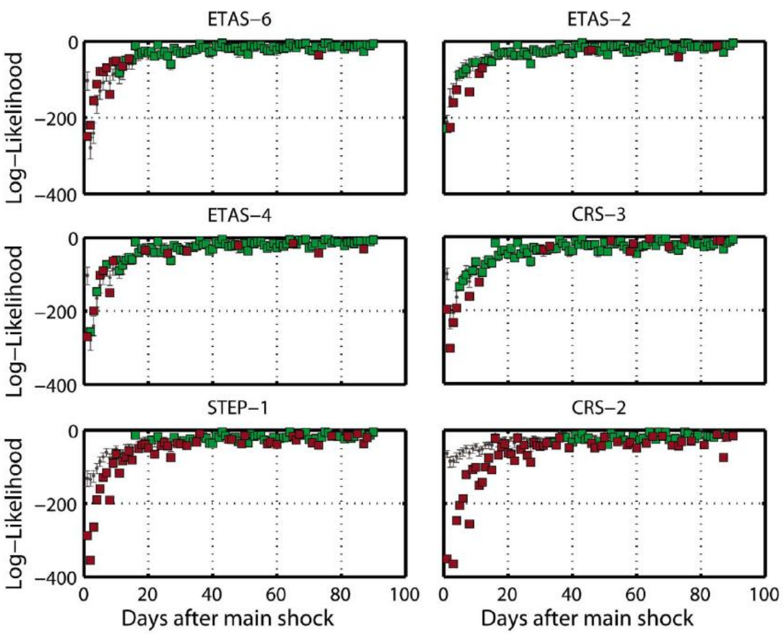


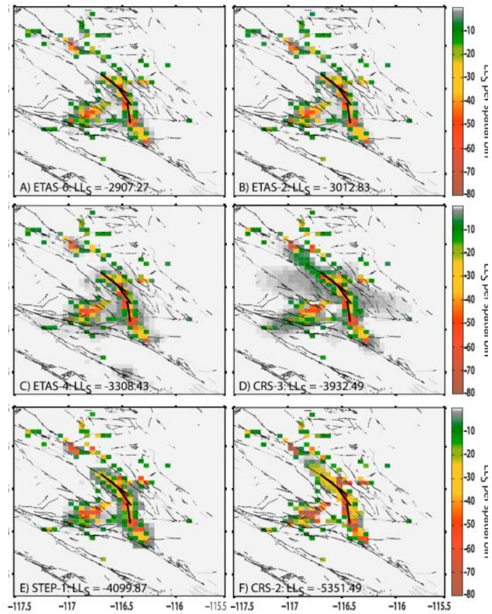


ıre 6. Map of log likelihood sum for each spatial bin (grid cell) at the end of the test lel names and joint log likelihood sum $LL_S$ (see Table 6) is given according to the L ETAS-6, (b) ETAS-2, (c) ETAS-4, (d) CRS-3, (e) STEP-1, and (f) CRS-2. Color scale i rated at $LL_S = -80$ for comparison reasons; light gray regions indicate log likelihood scores ero.

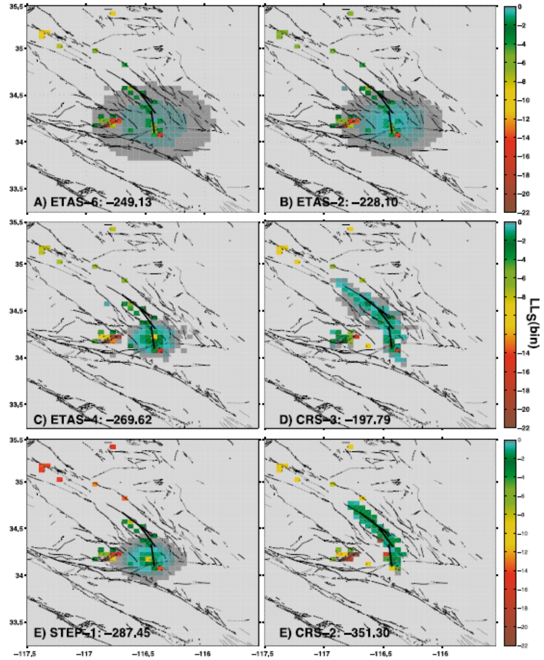


**Figure 7.** Map of log likelihoods for each spatial bin (grid cell) of test day 1. Model names and log likelihood sum $LL_S$(Day 1) of day 1 are given. Models are ordered as in Figure 6: (a) ETAS-6, (b) ETAS-2, (c) ETAS-4, (d) CRS-3, (e) STEP-1, and(f) CRS-2. Color scale is manually saturated at $LL_S = -22$ for comparison reasons; light gray regions indicate log likelihood scores very close to zero.

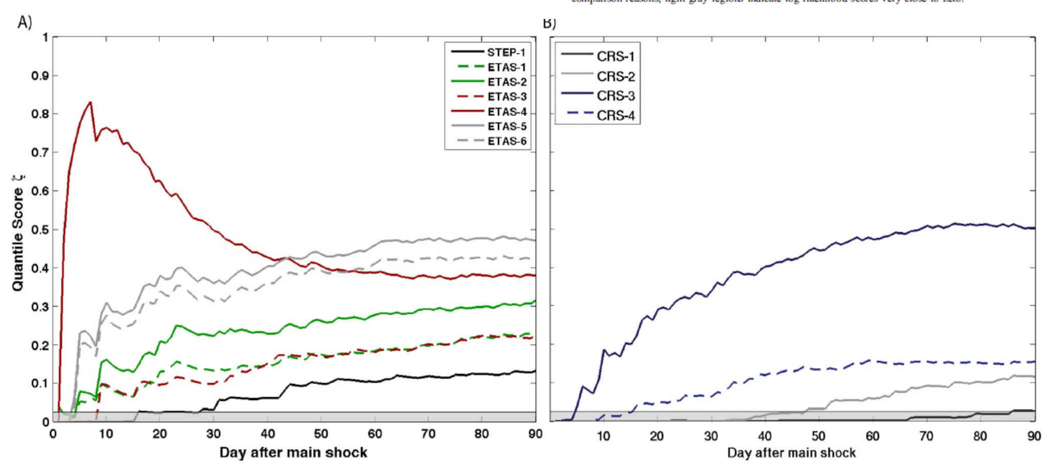


**Figure 9.** Quantile score $\zeta(t)$ for the cumulative S tests as a function of time for (a) CRS models and (b) statistical models. The significance level $\alpha_{eff} = 0.025$ is indicated as a gray patch at the bottom. In the time sequences, models ETAS-5, ETAS-6, ETAS-1, and ETAS-2, as well as CRS-3 are not rejected anymore after 5 days, followed by ETAS-3, CRS-4, STEP-1, CRS-2, and CRS-1.

**2013年2月 群馬県 日光地域 M6.3地震**

Omi et al., 2013 *Scientific Research*

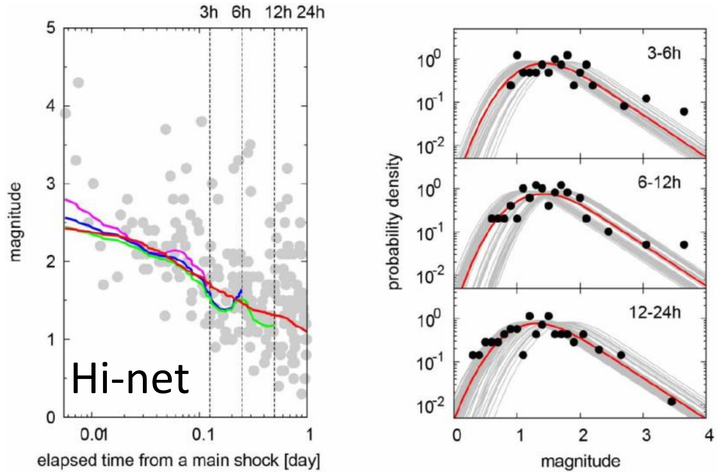


Figure S1 | Estimation of the time-dependent detection rate for the Hi-net catalog.

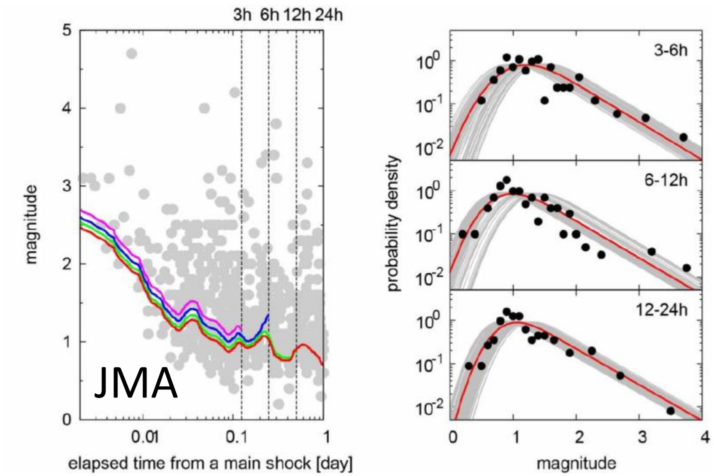


Figure S3 | Estimation of the time-dependent detection rate for the JMA catalog.

**2004年中越地震**

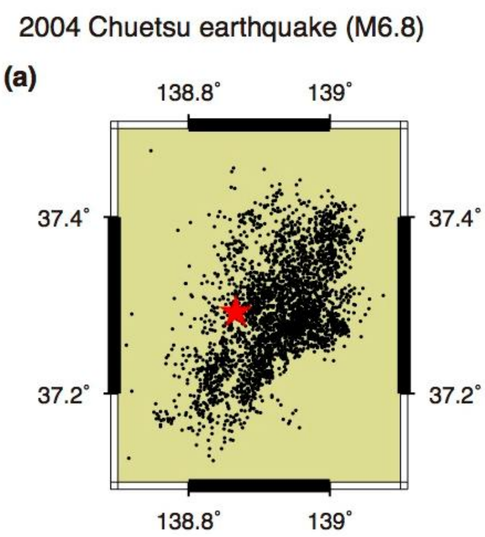


Omi et al., 2014 *GRL*

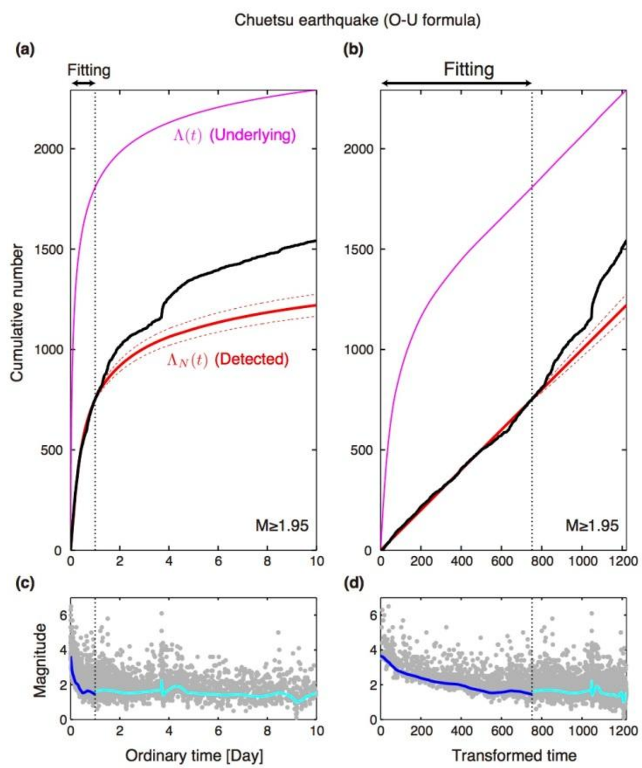


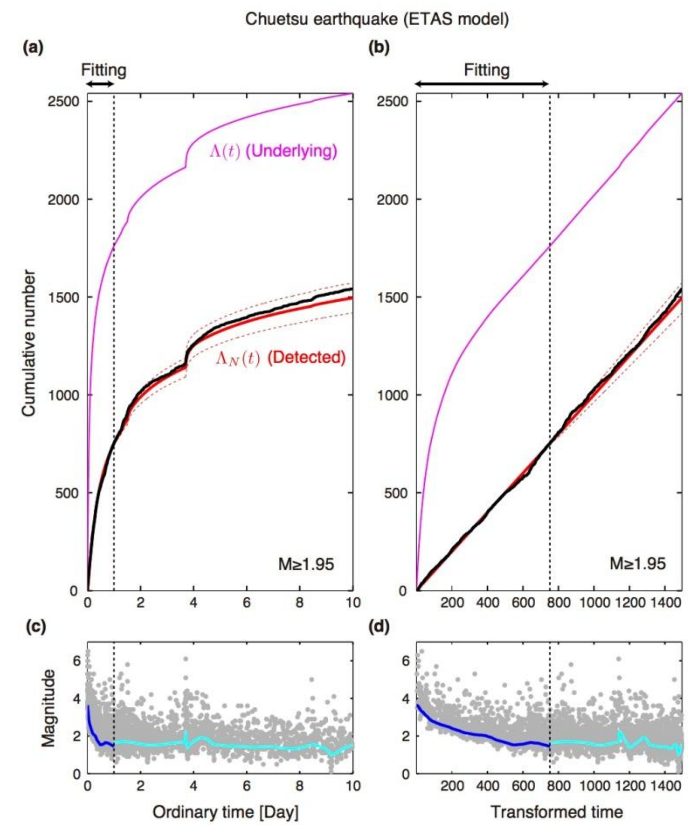

# 1980 Seismicity correlations

**Utsu (1975) 「Zisin」**

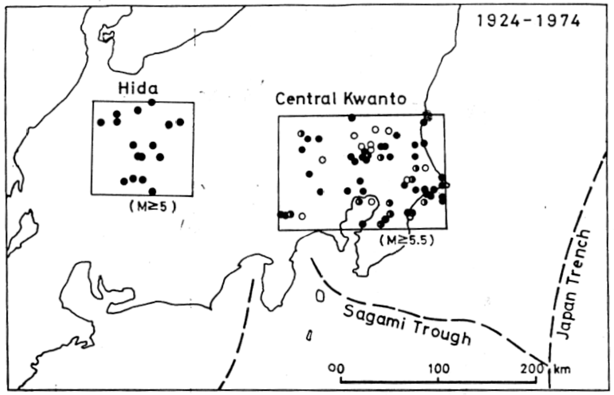


Fig. 1. Epicenters of 16 earthquakes in Hida and 61 earthquakes in central Kwanto. Filled and half-filled circles in the central rectangle indicate the earthquakes which occurred within ...ths and within one year from one of the Hida earthquakes, ...ely.

**(1981, 82)**

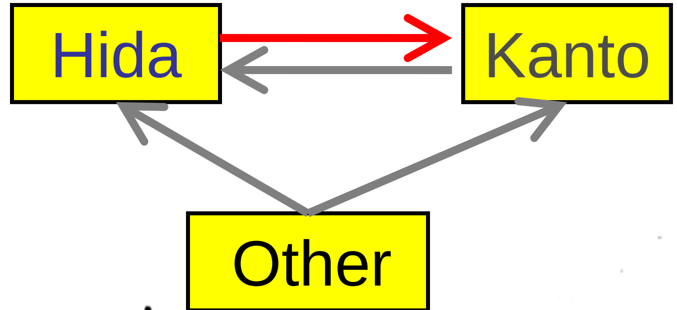


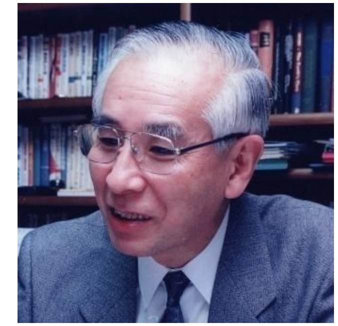


**seismicity = (trend) + (internal triggering) + (external triggering)**

$$\lambda(t \mid H_t) = \mu + \sum_{j=1}^{J} a_j t^j + \int_0^t g(t-s)\,dN_s + \int_0^t h(t-s)\,dM_s$$

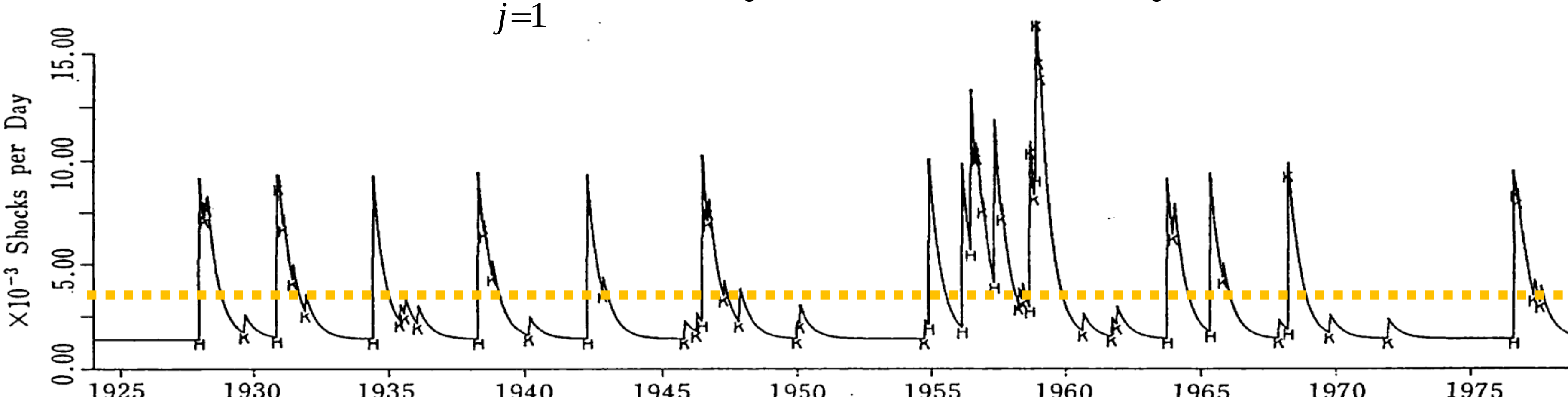

# seismicity = (trend) + (internal iriggering) + (external triggering)

(1982, 86, 99)

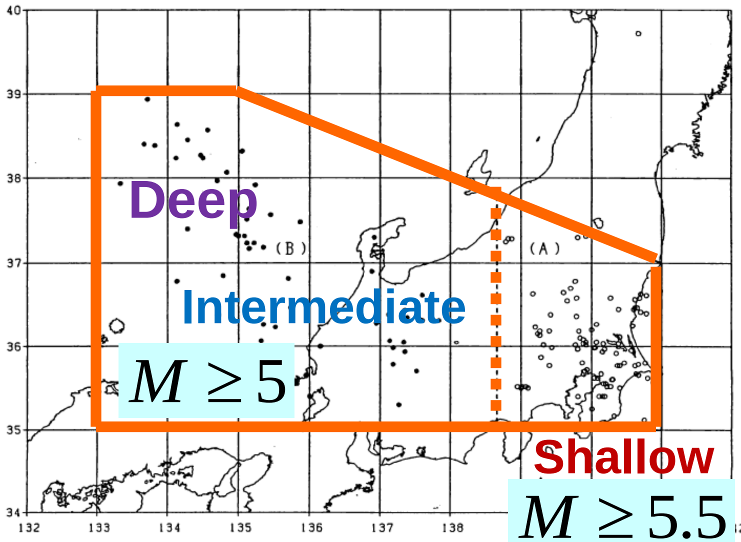


Figure 3. Spatial distributions of the shocks given in Table 6. Open circles and solid circles stand for the shallower and deeper shocks, respectively

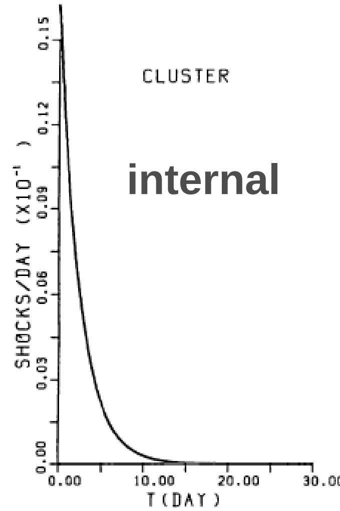


1ヶ月間

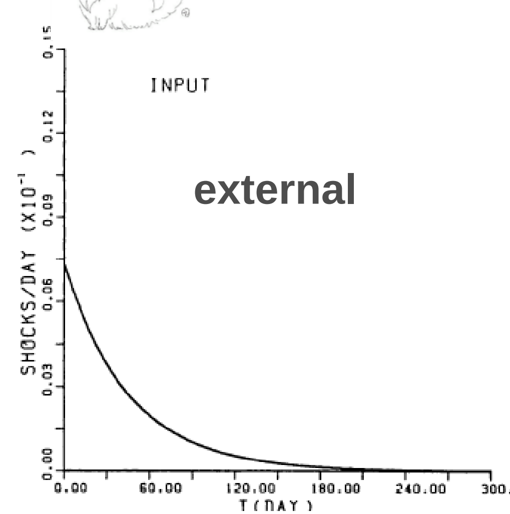


1年間

Shallow

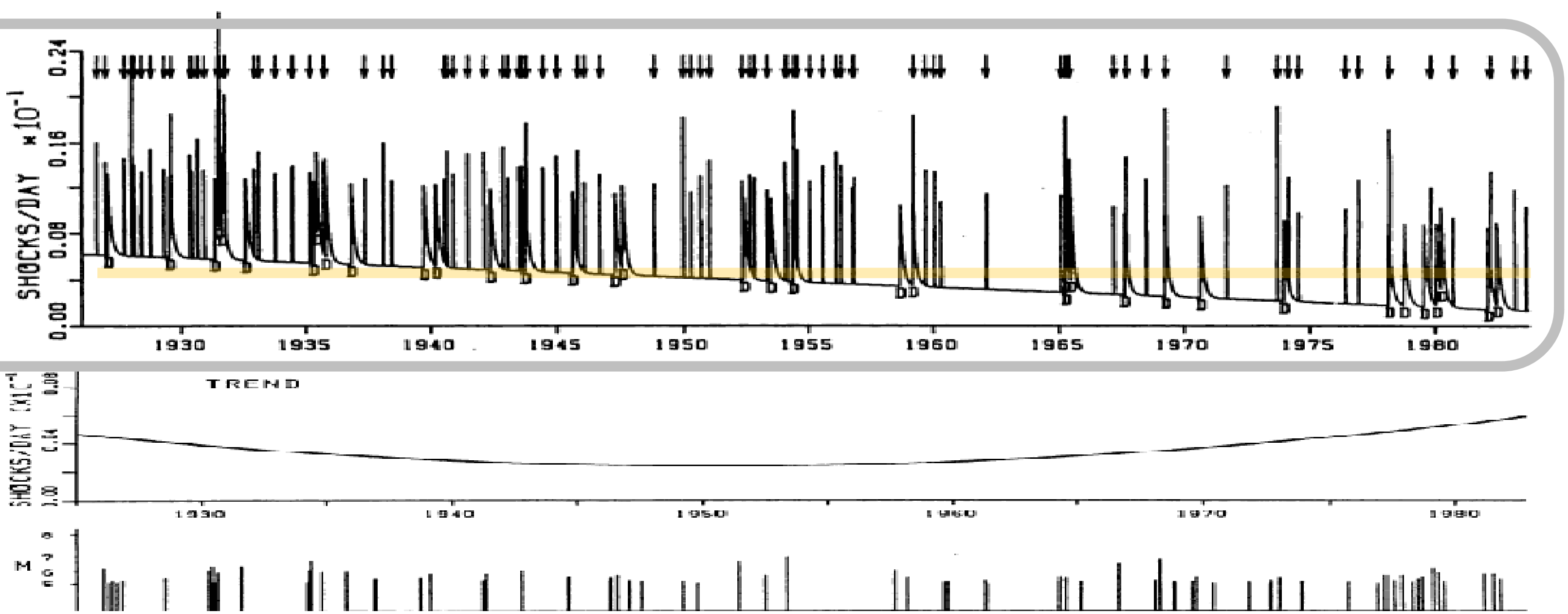


intermediate & deep

Zhuang et al. (2005, *PAGEOPH*)

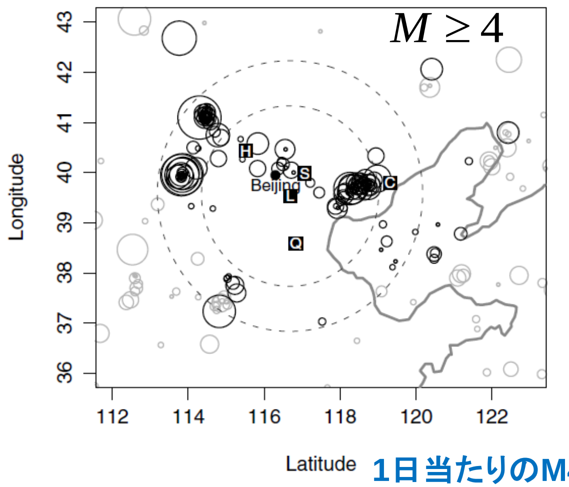


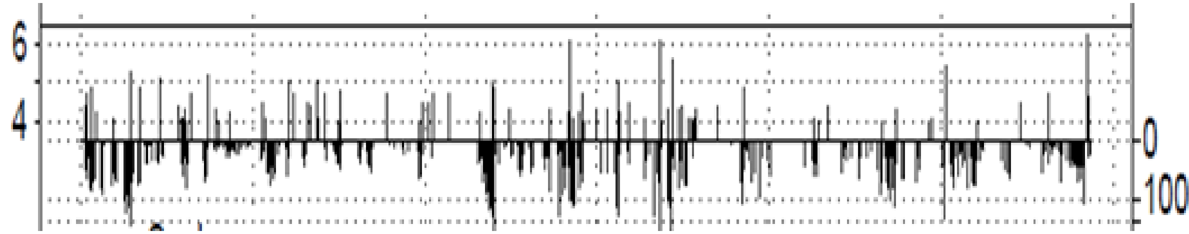


$$\lambda(t \mid H_t) = \mu + \int_0^t g(t-s)\,dN_s + \int_0^t h(t-s)\,dM_s$$

$$= \mu + \sum_{\{i;\, t_i < t\}} g(t-t_i) + \sum_{\{j;\, \tau_j < t\}} h(t-\tau_j)$$

1日当たりのM4以上の地震の発生率

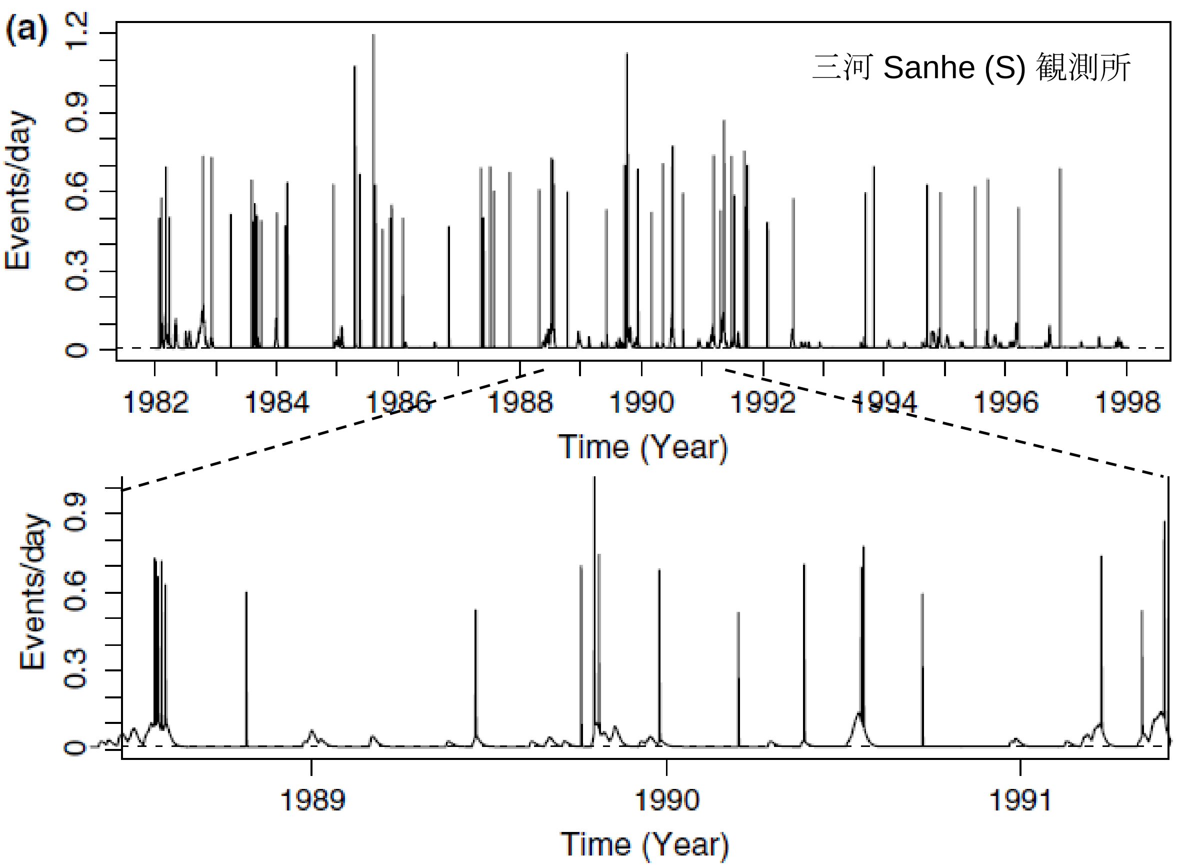


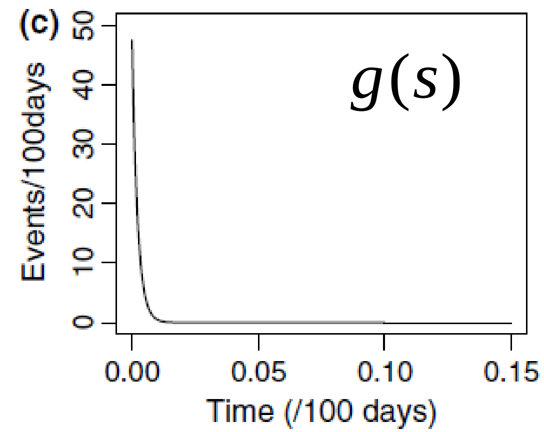


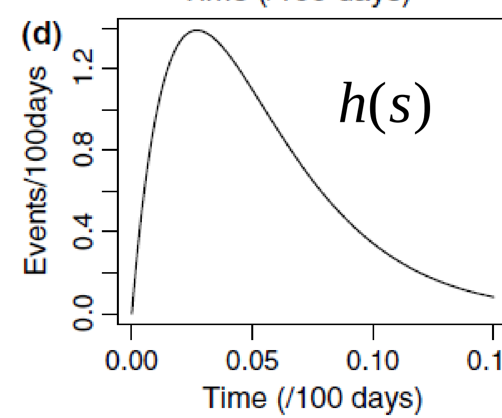

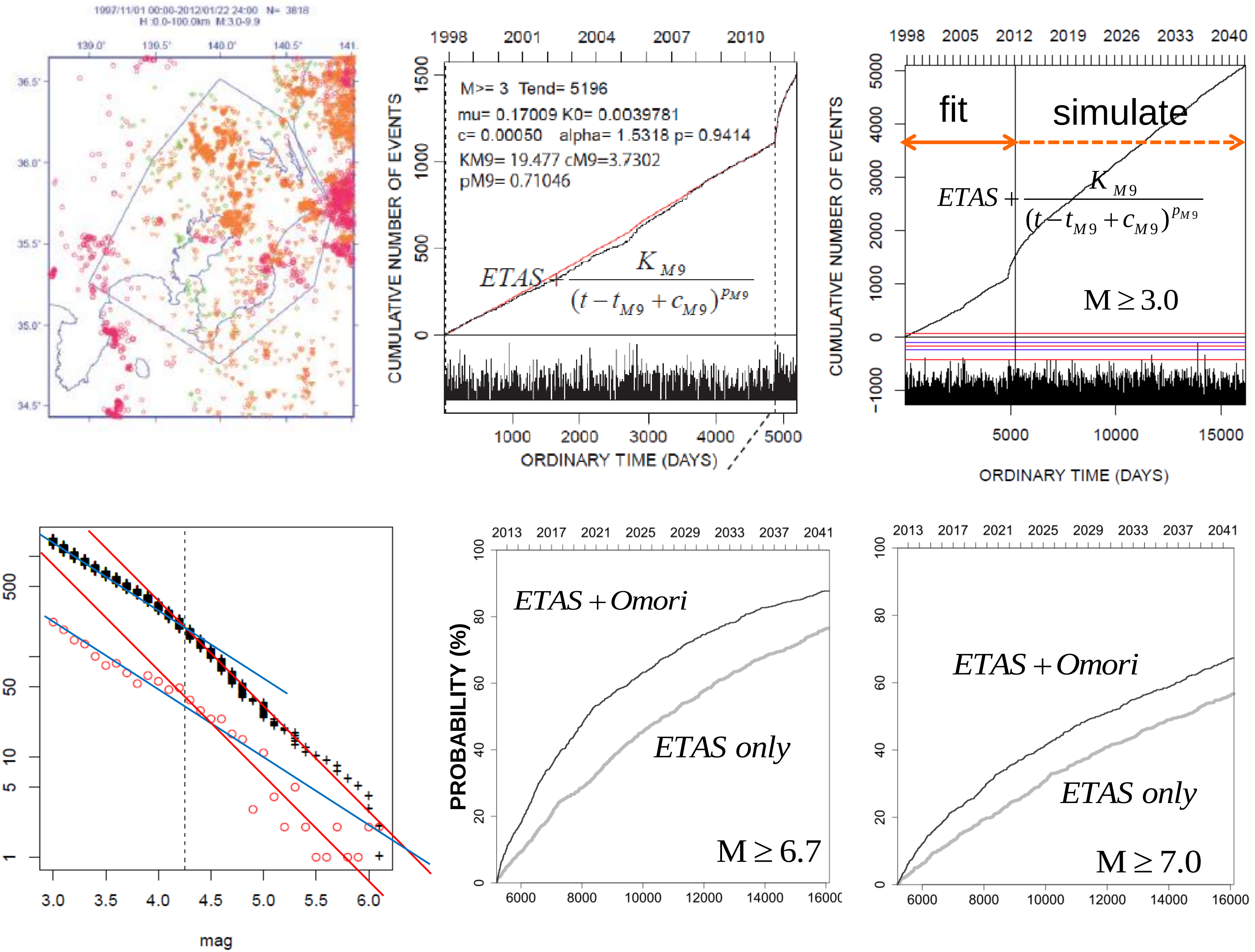

1997/11/01 00:00-2012/01/22 24:00 N= 3818
H :0.0-100.0km M:3.0-9.9
CUMULATIVE NUMBER OF EVENTS
M>= 3 Tend= 5196
mu= 0.17009 K0= 0.0039781
c= 0.00050 alpha= 1.5318 p= 0.9414
KM9= 19.477 cM9=3.7302
pM9= 0.71046
$ETAS + \frac{K_{M9}}{(t - t_{M9} + c_{M9})^{p_{M9}}}$
ORDINARY TIME (DAYS)
fit
simulate
$M \geq 3.0$
mag
PROBABILITY (%)
$ETAS + Omori$
$ETAS\ only$
$M \geq 6.7$
$M \geq 7.0$

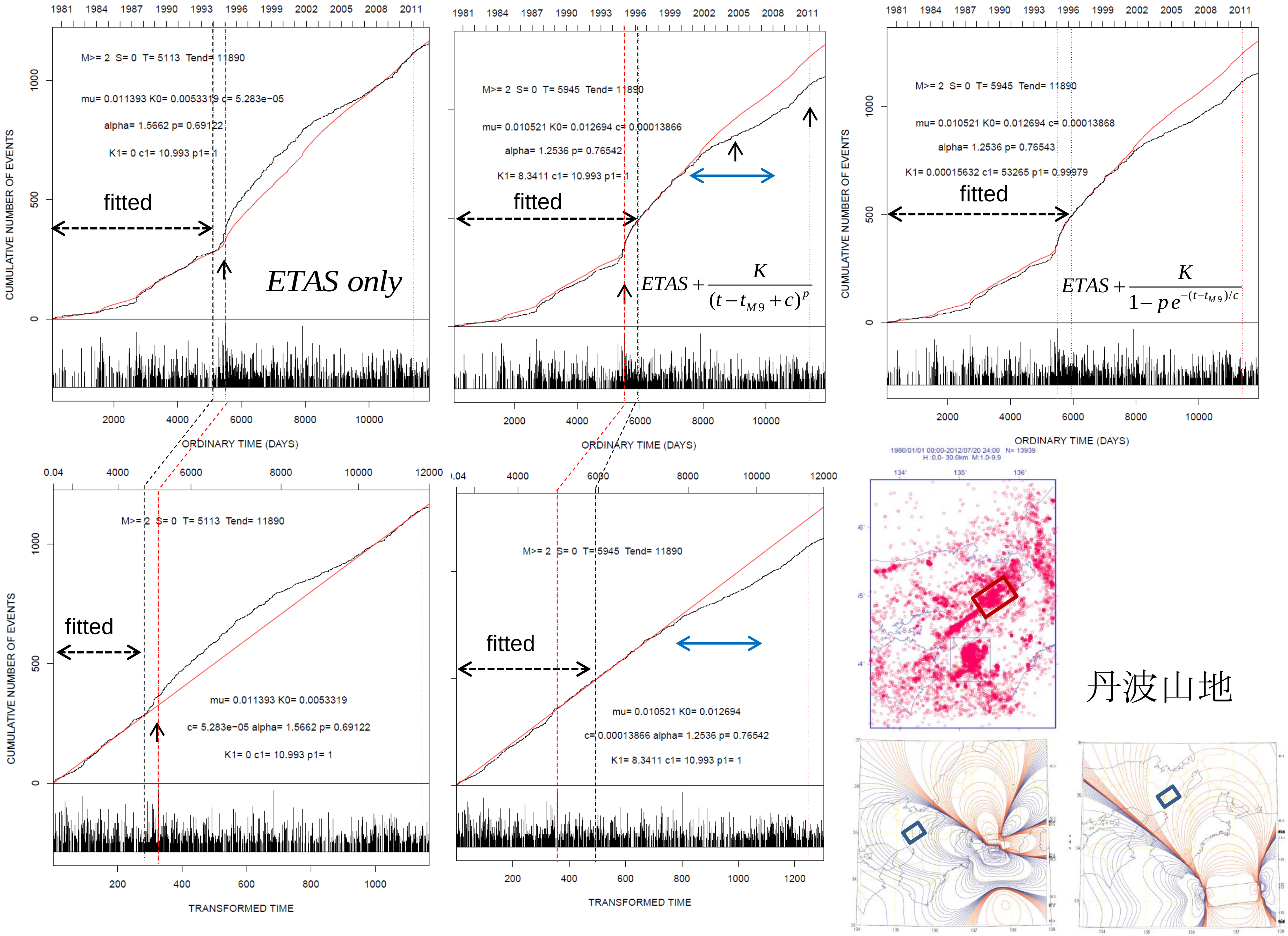

M>= 2 S= 0 T= 5113 Tend= 11890
mu= 0.011393 K0= 0.0053319 c= 5.283e-05
alpha= 1.5662 p= 0.69122
K1= 0 c1= 10.993 p1= 1
fitted
ETAS only
CUMULATIVE NUMBER OF EVENTS
ORDINARY TIME (DAYS)
M>= 2 S= 0 T= 5945 Tend= 11890
mu= 0.010521 K0= 0.012694 c= 0.00013866
alpha= 1.2536 p= 0.76542
K1= 8.3411 c1= 10.993 p1= 1
fitted
$ETAS + \frac{K}{(t - t_{M9} + c)^p}$
M>= 2 S= 0 T= 5945 Tend= 11890
mu= 0.010521 K0= 0.012694 c= 0.00013868
alpha= 1.2536 p= 0.76543
K1= 0.00015632 c1= 53265 p1= 0.99979
fitted
$ETAS + \frac{K}{1 - p e^{-(t - t_{M9})/c}}$
M>= 2 S= 0 T= 5113 Tend= 11890
fitted
mu= 0.011393 K0= 0.0053319
c= 5.283e-05 alpha= 1.5662 p= 0.69122
K1= 0 c1= 10.993 p1= 1
TRANSFORMED TIME
M>= 2 S= 0 T= 5945 Tend= 11890
fitted
mu= 0.010521 K0= 0.012694
c= 0.00013866 alpha= 1.2536 p= 0.76542
K1= 8.3411 c1= 10.993 p1= 1
TRANSFORMED TIME
1980/01/01 00:00-2012/07/20 24:00 N= 13939
H :0.0- 30.0km M:1.0-9.9
丹波山地

$$\lambda_\theta(t|H_t) \quad = \quad \textbf{(trend)} \; + \; \textbf{(Seasonality)} \; + \; \textbf{(triggering)}$$

$$= \mu + \sum_{j=1}^{J} a_j t^j + \sum_{k=1}^{K} \left\{ c_{2k-1} \cos \frac{2\pi k t}{T_0} + c_{2k} \sin \frac{2\pi k t}{T_0} \right\} + \int_0^t g(t-s) dN_s$$


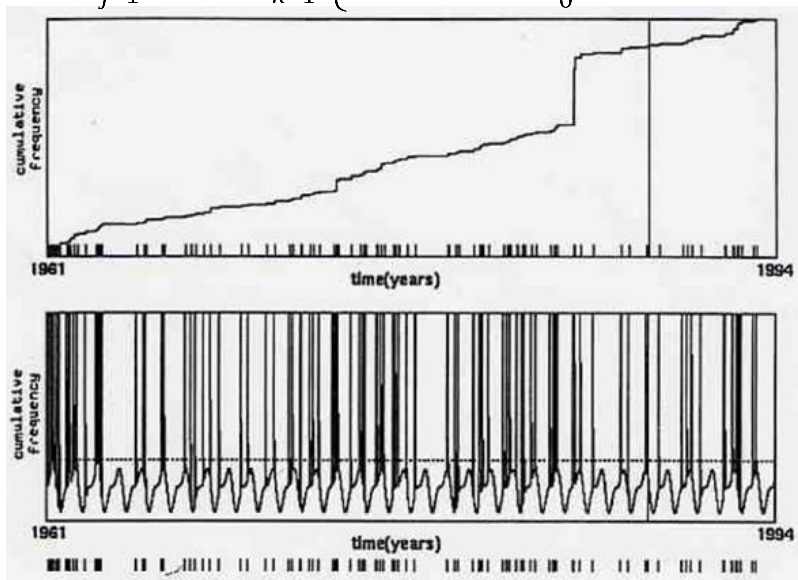



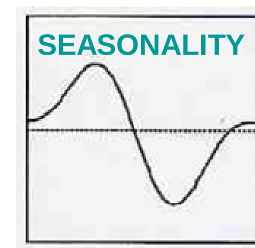


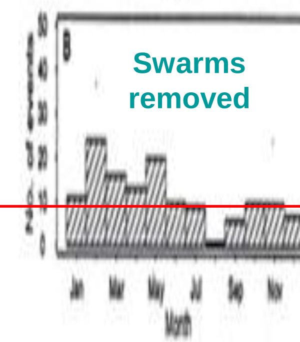


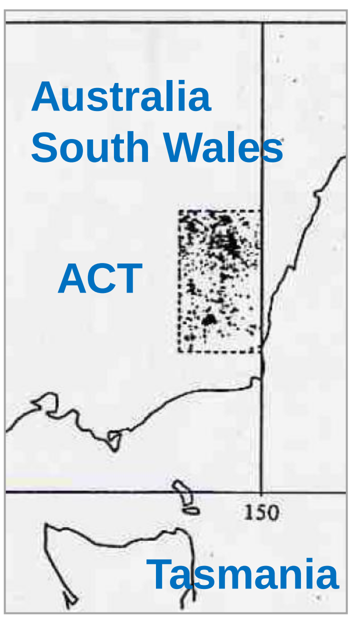


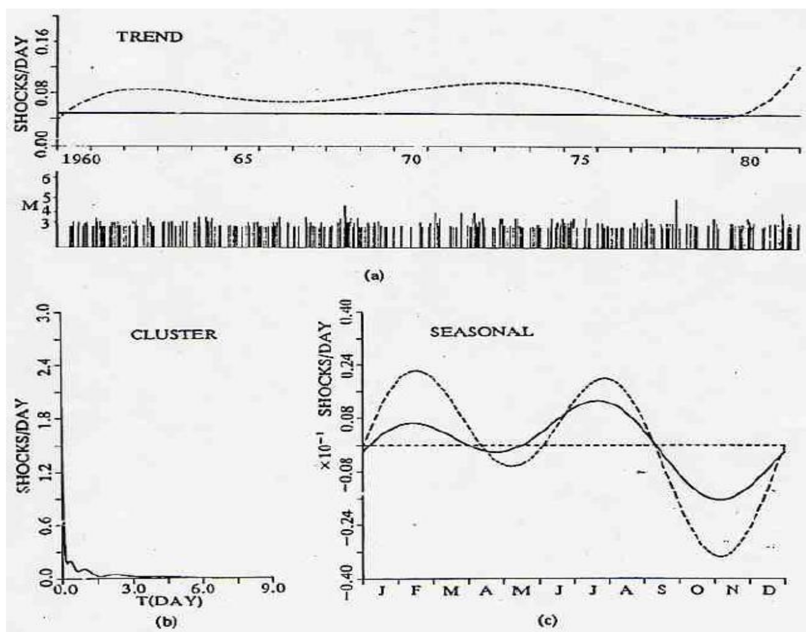


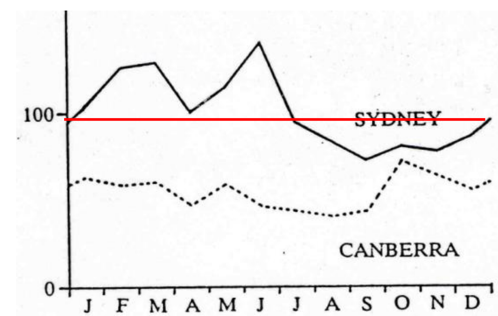


*Bull.ISI*, 1983; *J.App.Probab.*, 1986; *PAGEOPH*, 1999

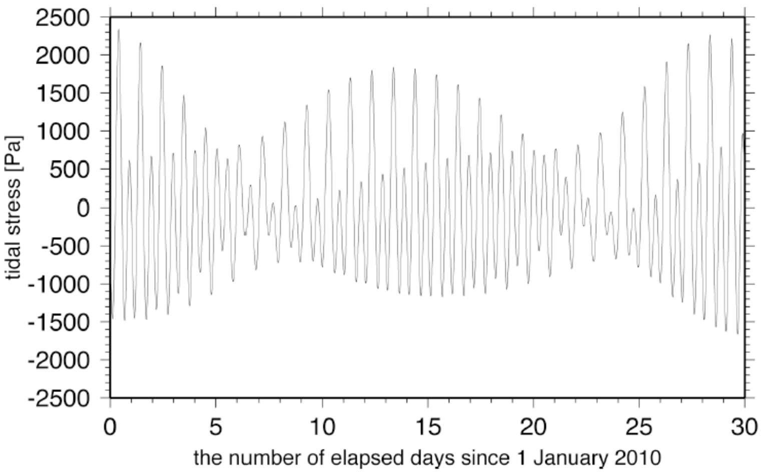


Iwata, T., and H. Katao (2006. *GRL*)

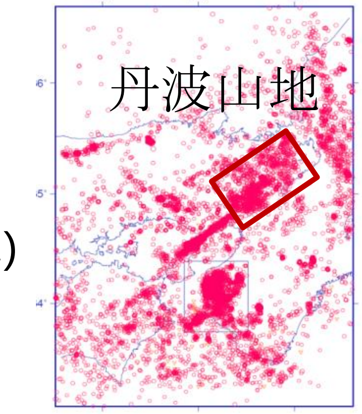


Tanaka, Ohtake, & Sato (2002; *JGR*. *GRL*)

$$\lambda(t) = \mu + (\text{trend}) + (\text{cluster}) + (\text{periodicity})$$

| Constraints | (i) | (ii) | (iii) | (iv) |
|---|---|---|---|---|
| $(N, L_1, L_2)$ | (3, 0, 0) | (3, 3, 0) | (3, 0, 3) | (3, 3, 3) |
| AIC | -4933.03 | -4938.83 | -4936.18 | -4942.14 |

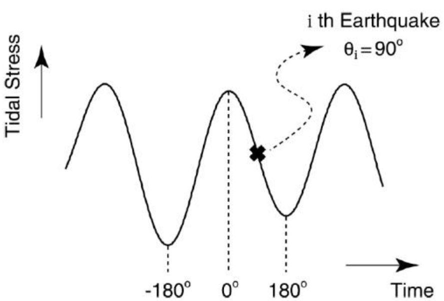


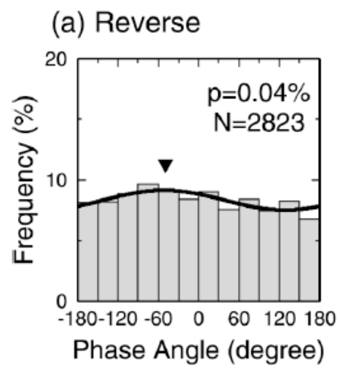


$$\lambda(t) = \mu + \sum_{k=1}^{N} a_k t^k + \sum_{i;t_i<t} \frac{K \exp(\alpha(M_i - M_z))}{(t - t_i + c)^p}$$
$$+ \sum_{k=1}^{L_1} A_{1k} t^{k-1} \cdot \sin\theta(t) + \sum_{k=1}^{L_1} B_{1k} t^{k-1} \cdot \cos\theta(t)$$
$$+ \sum_{k=1}^{L_2} A_{2k} t^{k-1} \cdot \sin(2\theta(t)) + \sum_{k=1}^{L_2} B_{2k} t^{k-1} \cdot \cos(2\theta(t))$$

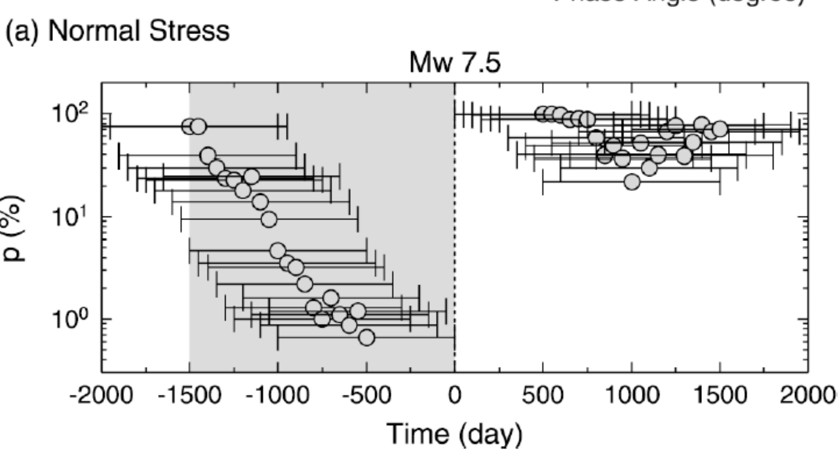


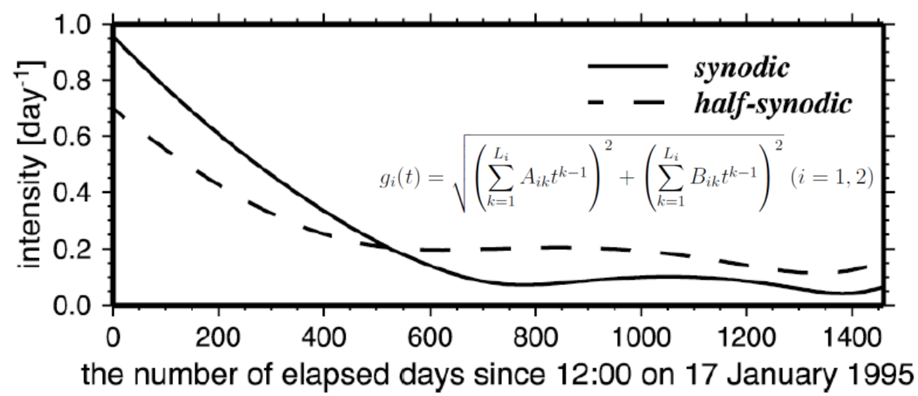

# まとめ

✎ 確率予測の予測能力は対数尤度で評価できる。データに当て嵌める統計モデルの選択やパラメータ推定は最大尤度法や**AIC**最小化によって予測力を上げることができる。

✎ 各地域に適した基準の地震活動の確率予測(長期·短期予測の相場のモデル)を与える（**CSEP**）。

→ 統計的点過程モデルの改訂を進める。

✎ 異常現象が、大地震の前兆なのか、どの程度切迫性があるのかなどの不確定さを見積もる。

→ 大地震の発生確率を、基準のものと比べて、この範囲、この期間、この程度まで増加·減少させる（確率利得）と言えるようになればよい 。これらを偏りなく見積もる必要がある。

→ 異常現象と大地震の因果性を記述する点過程モデルの作成

✎ 大地震を少しでも高い確率で予測するために、各種の観測データの有意な異常現象を多数考慮して、統計モデルで確率利得を高め、複合的に予測することが有力である。

→ 異常現象の複合性を記述する点過程モデルの作成